Printed transducers embedded in polymer coatings

H. Enser, J. K. Sell, P. Kulha, W. Hilber, B. Jakoby OVE

We provide an overview on our recent work on embedded printed transducers. This includes the description of appropriate technologies as well as technological considerations for the integration of sensors and actuators into polymer coatings, e.g., of sheet metal. In particular, the integration of capacitive large area sensors, piezo- and pyroelectric layers, and strain gauges is discussed. The devised concept has the potential to introduce additional functionality to a variety of products without the need of significant changes to associated production processes.

Keywords: printed transducers; embedded transducers; printed sensors; industrial application; organic coatings; functionalized coatings

Gedruckte Messwertwandler, eingebettet in Polymerbeschichtungen.

Die Autoren geben in dieser Arbeit eine Übersicht über ihre jüngsten Arbeiten betreffend gedruckte eingebettete Messwertwandler. Sie präsentieren geeignete Herstellungstechnologien und betrachten die Einbettung von Sensoren und Aktoren in Polymerbeschichtungen, z. B. auf Blechen. Im Speziellen wird die Integration großflächiger Sensorstrukturen, piezo- und pyroelektrischer Schichten sowie gedruckter Dehnungsmessstreifen diskutiert. Das erarbeitete Konzept hat das Potential, zusätzliche Funktionalitäten in eine Reihe von Produkten, ohne signifikanten Mehraufwand in der Produktion, zu integrieren.

Schlüsselwörter: gedruckte Sensoren; gedruckte Messwandler; eingebettete Sensoren; industrielle Anwendungen; organische Beschichtungen; funktionalisierte Beschichtungen

Received May 25, 2018, accepted June 30, 2018, published online August 23, 2018

1. Introduction

In recent years, much attention has been devoted to the development of functional inks and pastes. As a consequence, a variety of nano-particle and flake-based inks and pastes (including silver and carbon) and conductive polymer inks and pastes (e.g., poly(3,4-ethylenedioxythiophene) polystyrene sulfonate, short PEDOT:PSS) are currently available commercially. These materials can be used in additive deposition processes, e.g., ink jet printing, gravure offset printing, flexographic printing, screen printing or spray coating and enable the realization of printed electronics and transducers, e.g., polymer solar cells [1], OLEDs [2], RFID antennas [3, 4], piezoelectric sensors [5] capacitive gas sensors [6] or strain gauges [7]. Compared to semiconductor fabrication processes, the printing technology is cost effective and enables a rapid transfer of new designs from laboratory to fabrication. In general, polymeric foils, glass or coated papers are used as substrate for printed electronics. The final printed circuitry and components are integrated into a product in successive assembly steps. In the contributions discussed in this paper, we refrained from using a dedicated substrate but used the surface of an existing product as substrate instead. This approach has the advantage that no further assembly steps are necessary and that no additional adhesive/adhesion layer is required. Furthermore, a variety of transducers can be embedded in virtually every surface, which can be coated. As an example of the proposed concept, we illustrate the realization of printed embedded transducers on organic coated sheet steel. Figure 1 shows an example of a fabricated device (strain gauge). In the following sections, the technology and the associated requirements are discussed followed by three examples for sensors, i.e. capacitive sensors, strain gauges, and piezo/pyroelectric sensors. Details of this research have been previously presented in conference proceedings [8–12].

2. Sheet metal as substrate

For demonstrator purposes, sheet metal with a thickness ranging from 0.5 mm to 2 mm is used as a substrate as depicted in Fig. 1. The sheet metal is primed with a polyurethane or polyester primer with a thickness of between 5 µm and 20 µm. Due to the inherent surface roughness of the used sheet metal and the pigmentation of the applied primers, the surface roughness of the substrate (given by the root-mean-squared deviation) is in the range of 1 µm. This is orders of magnitude higher than on other substrates normally used for the realization of printed transducers [9] and thus particularly challenging. The high surface roughness impedes the printing of very thin conductive layers and excludes certain applications of printed electronics, like, e.g., OLEDs (organic light emitting diode), which require uniform, defect-free layers with well-defined thicknesses. On the other hand, uncoated paper, in general, is rougher

Enser, Herbert, Institute for Microelectronics and Microsensors, Johannes Kepler University Linz, Altenberger Straße 69, 4040 Linz, Austria (E-mail: herbert.enser@jku.at); **Sell, Johannes K.,** Institute for Microelectronics and Microsensors, Johannes Kepler University Linz, Altenberger Straße 69, 4040 Linz, Austria and now with voestalpine Stahl GmbH Linz, Linz, Austria; **Kulha, Pavel,** Department of Microelectronics, Czech Technical University, Prague, Czech Republic; **Hilber, Wolfgang,** Institute for Microelectronics and Microsensors, Johannes Kepler University Linz, Altenberger Straße 69, 4040 Linz, Austria; **Jakoby, Bernhard,** Institute for Microelectronics and Microsensors, Johannes Kepler University Linz, Altenberger Straße 69, 4040 Linz, Austria

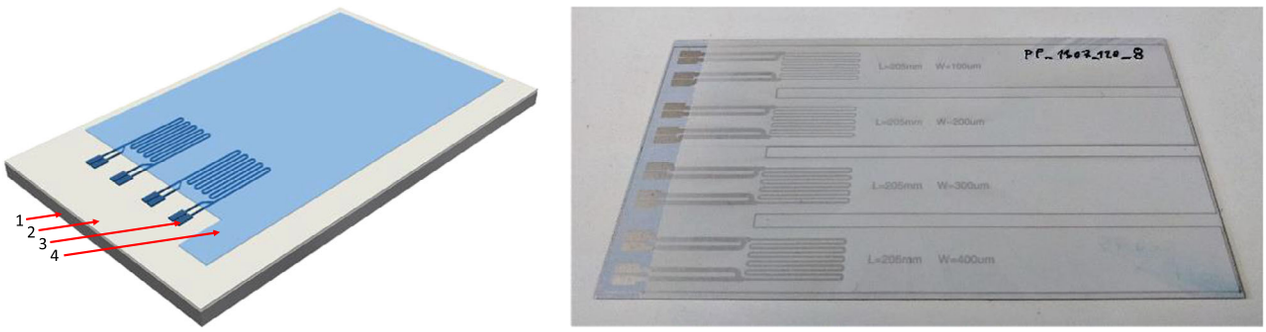

Fig. 1. Schematic of printed strain gauges (3) on top of organically precoated (2) sheet steel (1), with an additional top coating layer (4) for mechanical protection and stabilization. The sensor layer (3) is fabricated either with screen-printing (for silver and carbon black) or deposited via PVD (physical vapor deposition) (for gold). The photo on the right shows an example of a demonstrator featuring a silver-based strain gauge. In this case the top coating is thin enough to provide a view on the underlying sensor structures

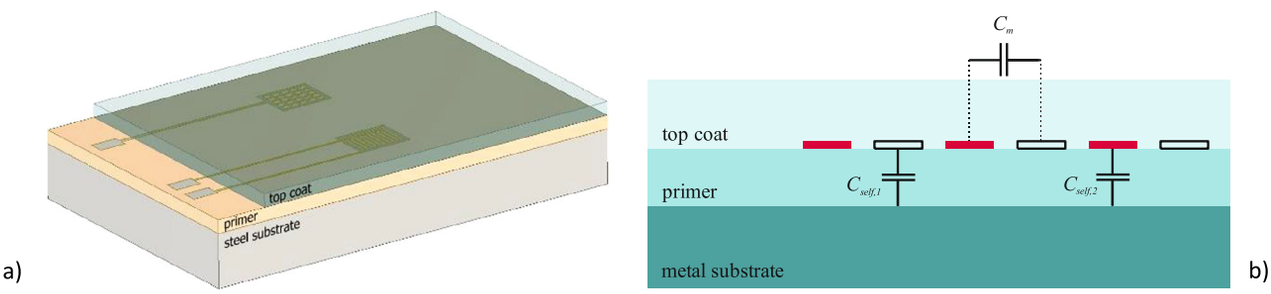

Fig. 2. (a) Schematic layout of self (left) and mutual (right) capacitance based buttons; (b) cross section of a mutual capacitance-based button with capacitive coupling schemas. The red and black electrodes symbolize the two interdigital finger electrodes as see in (a)

than the organic primer layer. Despite of its rough surface, many applications, including light emitting electrochemical cells [13] and loudspeakers [14], have been realized on uncoated paper. Further examples for printed electronics on paper are given in [15]. The chemical and physical properties of the primer layer are crucial for the selection of printing materials. The surface energy of the primers used on the metal sheets is in the range between 28 mN m^{-1} and 33 mN m^{-1}. This is well below the surface energy of substrates commonly used for printed electronics, e.g., PET (polyethylene terephthalate) or polyimide [16] which both feature surface energies close to 40 mN m^{-1}. For appropriate wetting of the substrate during processing, it is crucial that the surface tension of the ink or paste is close to the surface energy of the primer. Commercially available ink and paste formulations are typically designed for the application on the above-mentioned standard substrates. Therefore, wetting and adhesion problems can occur and have to be investigated thoroughly before further application. Furthermore, the chemical resistance of the primer to the inks or pastes solvent has to be taken into account. The primer itself is thermally cross-linked and stable towards most solvents. However, solvents can still introduce swelling of the primer, which may result in a loss of adhesion to the metal substrate.

3. Printing technology

Printing is an additive manufacturing technology that can easily be scaled from lab-to-fab and enables the low cost mass production of electronic components. A comprehensive review of the technologies used for printed electronics and their unique properties (resolution, printing speed, layer for the fabrication of sensors and electronics) is given in [17]. The prototypes shown exemplarily in this work are fabricated using flatbed screen-printing. The used silver pastes (LOCTITE ECI1010 and LOCTITE EDAG PF 050) and the carbon paste (LOCTITE EDAG PR 406B) were received from Henkel, the PEDOT:PSS paste ORGACON EL-P3155 was obtained from AGFA and the P(VDF-TrFE) formulation was kindly provided by Johanneum Research [5].

4. Capacitive sensors on steel

We reported the realization of embedded capacitive sensors on steel substrate previously in [9]. As illustrated in Fig. 2, capacitive sensors can either be based on sensing the self-capacitance, i.e., the capacitance between sensor and the conductive substrate C_{self}, or the mutual capacitance C_m, i.e., the capacitive coupling between two conductive structures (e.g., interdigital electrodes). For a large area application of embedded capacitive sensors on metallic substrates, several challenges have to be met. One of these challenges is the low thickness of the isolating primer layer and its high electric permittivity. Applied to a 20 µm primer, the self-capacitance per area is in the order of 300 pF/cm^2. For a large area sensor, the thus formed offset in the self-capacitance may exceed the desired change of the self-capacitance due to an interaction (i.e. the sensor effect) by orders of magnitude. Therefore, it may be difficult to resolve a sensing event and, thus in general, it is advisable to use the mutual capacitance for the realization of large area capacitive sensors. Another important aspect, which has to be considered for the realization of large area sensors, is the resistivity of the printed conductors. The associated resistivity in connection with the capacitances results in a low-pass behavior. This limits the sensitivity and affects the response dynamics. Thus for large area sensors, metal based polymer nanocomposites featuring higher conductivies are considered preferable A schematic

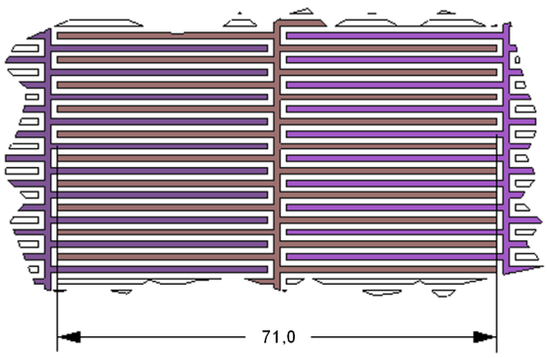

Fig. 3. Schematic description of the general layout of a large area capacitive sensor. The structure is repeated over an area of 260 mm × 1200 mm. The gap and the line width are 1 mm

implementation of a prototype large area capacitive sensor can be seen in Fig. 3. It is based on interdigital electrodes with a line width and a gap of 1 mm each. This pattern is repeated over an area of 260 mm × 1200 mm. In the prototype application, each electrode is 71 mm wide (see Fig. 3). This width is a tradeoff between the number of channels required for the readout of the sensor and the spatial resolution in horizontal direction. Depending on the available readout options, this value can be adjusted to the requirements of the target application. Large area sensors were manually screen-printed with a conductive silver paste (Henkel ECI1010) on a primed steel substrate with a primer thickness of 20 µm. A polyester mesh (SEFAR PET 1500) with a mesh number of 120/305-34 was used for the screen. The paste was cured in a continuous furnace at 110 °C. The electric characterization of the sensor was performed without further top coating of the sensor. Instead, the sensor area was covered with two sheets of plastic foil with a total thickness of approximately 40 µm. The self-capacitance of the electrodes and the mutual capacitance of adjacent electrodes were determined with an Agilent 4294A impedance analyzer. For the measurement of the mutual capacitance, the steel substrate was connected to ground. Exemplarily, the self-capacitance of one of the electrodes and the mutual capacitance with an adjacent electrode is depicted in Fig. 4 where the capacitance was calculated from frequency dependent impedance data. The large offset of the self-capacitance can be clearly seen. In addition, the calculated capacitance significantly varies at higher frequencies (above a few kHz) indicating that a simple capacitor model is insufficient to represent the impedance at these frequencies. The shift of the capacitance introduced by placing a finger on the sensor structure is shown in Fig. 5. The capacitance was determined using the impedance analyzer at 5 kHz. For the given thicknesses of the sensor structure, primer, the self-capacitance increases by about 20 pF when attaching a cover foil. The associated change of the mutual capacitance is in the order of 5 pF. The offset capacitance of the mutual capacitance is only 11 pF whereas the offset capacitance of the self-capacitance measurement is in the range of 56 nF. Therefore, despite the higher absolute value, resolving the changes of the self-capacitance with the impedance analyzer is more difficult than resolving the changes of the mutual capacitance and additionally requires significantly more averaging of the data in order to achieve a reasonable sensor signal.

5. Embedded strain gauges

Strain gauges are widely used for the measurement of force, strain, and torque in components that are subjected to mechanical stress. Using printing techniques, sensor implementations based on

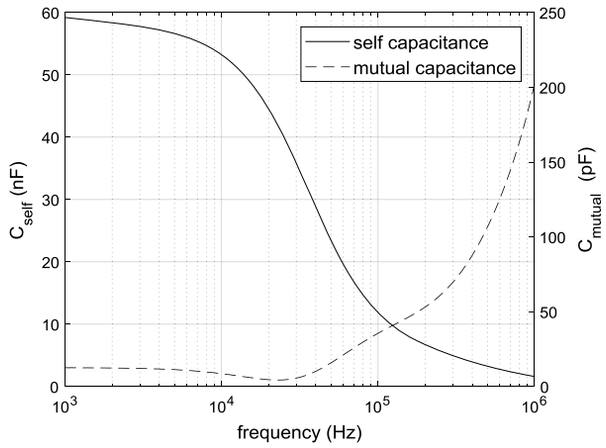

Fig. 4. Self-capacitance (left) of an electrode and mutual capacitance (right) of the same electrode with an adjacent electrode

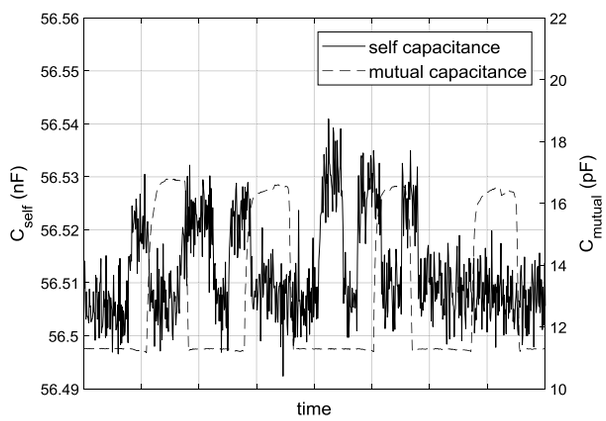

Fig. 5. Influence of a finger on the (left) self-capacitance and (right) mutual capacitance of a large area capacitive sensor. The capacitance was measured at 5 kHz with an Agilent 4294A impedance analyzer

graphite [18], silver [19], PEDOT:PSS [20], and carbon nanotubes [21] have been demonstrated. In general, these strain gauges have been fabricated on polymeric substrates, e.g., polyimide [22], polyamide [20], or poly-dimethyl-siloxane (PDMS) [17]. All these sensors have in common that the strain gauge is fixed to a test device by an adhesive layer. This adhesive layer impedes the direct measurement of strain on the test device, as the mechanic properties of the adhesive are important for the perception of strain on an attached sensor. This issue can be solved by directly printing of a strain gauge sensors, with a sheet thickness of 3 µm for silver based and 14 µm for carbon black based strain gauges, onto the surface of a test device [23, 24]. Meander-shaped strain gauges were embedded into the organic coating of sheet steel, which has a thickness of 0.8 mm as outlined in [24]. The response of such an embedded carbon based strain gauge can be seen in Fig. 6. For the characterization of the sensor, the steel substrate was clamped at one side. The strain gauge was positioned at the clamped edge where the maximum strain is imposed by a deflection on the other end of the steel substrate, occurs. The end of the steel substrate was deflected by ±5 mm using a motorized stage. To ensure temperature stability during the measurements, the sample was placed in a climate chamber at 25 °C and 50% relative humidity. The resistance of the sensors was recorded over 172 deflection cycles with a Keithley DMM7510 multimeter.

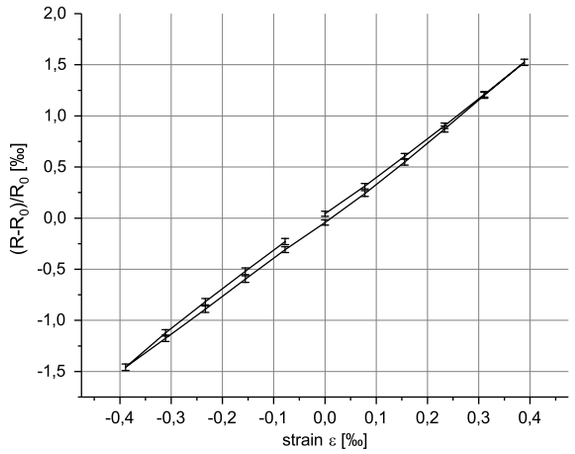

Fig. 6. Strain dependence of an embedded strain gauge that has been screen-printed with carbon polymer thick film ink (Henkel Electrodag PR-406B). The response of the sensor was averaged over 172 deflection cycles. The standard deviation is indicated by error bars. The sensor features a gauge factor of 3.8

In the following, we briefly address the three spurious effects that were observed during the characterization of the strain gauge samples for both, silver-based strain gauges as well as carbon black based ones. First, a set in effect is clearly present. Second, a non-linear response for tensile as well as compressive strain can be observed, including a presented solution to stabilize the effect. Third, a hysteresis was observed for all samples. All measurements discussed in the following paragraph are conducted under controlled environmental conditions in a climate chamber WKL 100 from Weiss Technik. The parameters were set to 25 °C for temperature and minimum humidity, which, according to the datasheet, corresponds to 25% RH at 25 °C.

Figure 7 depicts one hundred measurement cycles of the silver-based strain gauge. One measurement cycle is defined as a movement of +5 mm to impose compressive strain onto the strain gauge, followed by a movement of −10 mm to reach a −5 mm position and thus impose tensile strain resulting in 20 measurement points per cycle. It is clearly observable that after the first 10 cycles the silver-based strain gauge is more or less stabilized. In comparison to silver, carbon black based strain gauges, as can be seen in Fig. 8(a) showing the initial 100 cycles, need at least 90 cycles until the sensor response can be presumed stable. To confirm this behavior, the same sample with carbon black was measured for a second time; again for 100 cycles. Figure 3(b) depicts the second run for carbon black; it shows that the sensor response has stabilized significantly and no set-in effect can be observed.

Furthermore, the influence of sensor fabrication on the nonlinearity as well as a hysteresis of the gauge factor was investigated. Since the sensor pattern is printed on top of a polymer-based coating, it is observed that the initial sensor response to compressive as well as tensile strain is only linear in a very narrow deflection range. A more detailed investigation revealed that some of the non-ideal properties are also related to the used materials (e.g., substrate and coating). However, in an additional step, a second layer of polymer based protective coating is applied on top of the sensor structure. First, this is done because the double layer protective coating serves as a corrosion protection, but the intention is also to protect the thin sensing layer mechanically.

After application of this protective layer, another measurement run was carried out to see if this additional temperature treatment has an effect on the sensor layer. Surprisingly, not only an effect on the sensitivity of the strain gauge was found, but also that the second layer of polymer protection eliminated the nonlinearities. The second measurement run is depicted in Figs. 9(a) and 9(b).

One can observer that the Hysteresis does not improve with the addition of a top coat, also visible with the top-coated gold reference sample depicted in Fig. 9(a). The non-linear response on the other hand is significantly reduced with the mechanically stabilizing top coat also depicted in Fig. 9(b). We assume that from the comparison between an uncoated a top coated as well as a metal evaporated gold reference sample it is viable to deduct the fact that

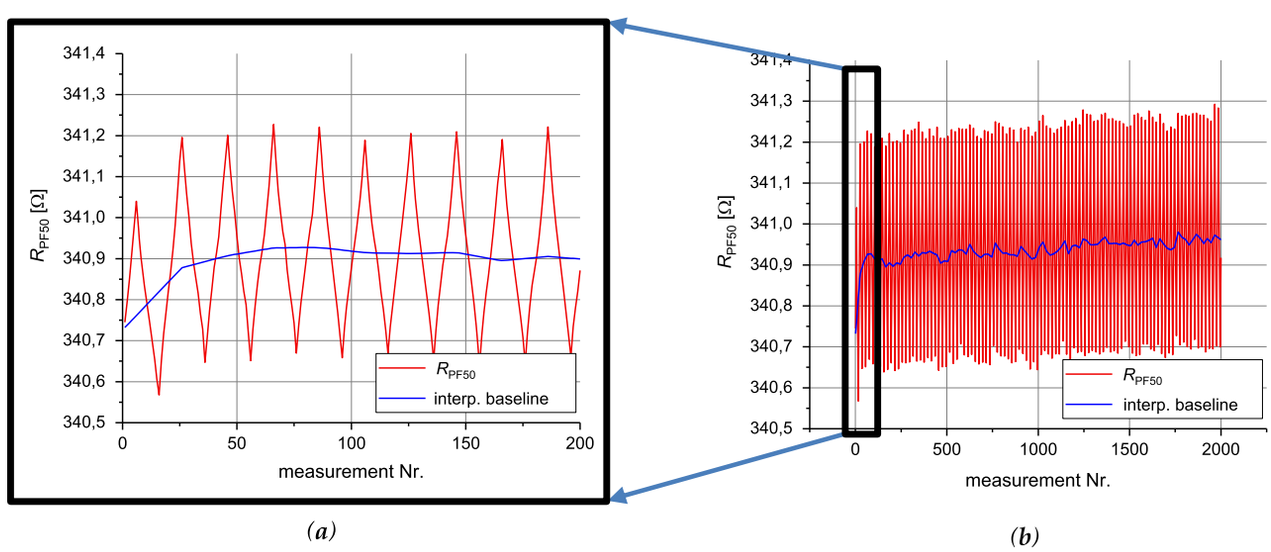

Fig. 7. (a) Zoom into the first 200 measurement points, corresponding to ten full cycles of compressive and tensile strain© of 4.5 × 10.4. Baseline shows set-in after six cycles. (b) Long-term measurement of 100 cycles for printed silver (PF50) based strain gauge at a constant temperature of 25 °C and 25% RH in a Weiss Technik WKL 100 climate chamber. The long-term baseline still shows some kind of drift, but the initial set-in effect settles after six cycles

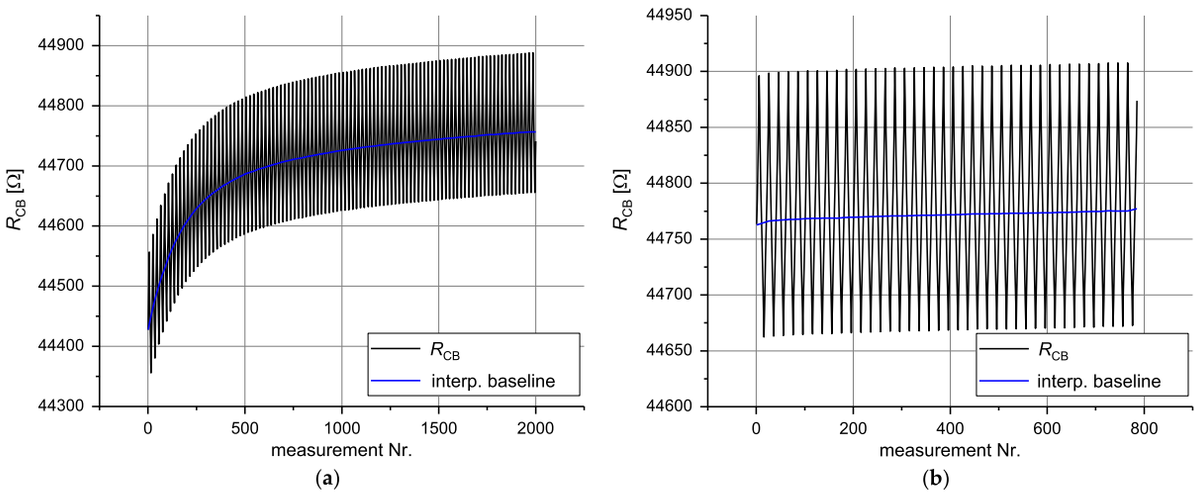

Fig. 8. (a) Long-term measurement of 100 cycles for carbon black based strain gauge at a constant temperature of 25 °C and 25% RH in a climate chamber. Only after about 90 out of 100 cycles, where one cycle amounts to 20 data points, the gauge factor becomes more stable. (b) Second long-term measurement for the same carbon black sample as in (a). The second run shows that the set-in period is completed

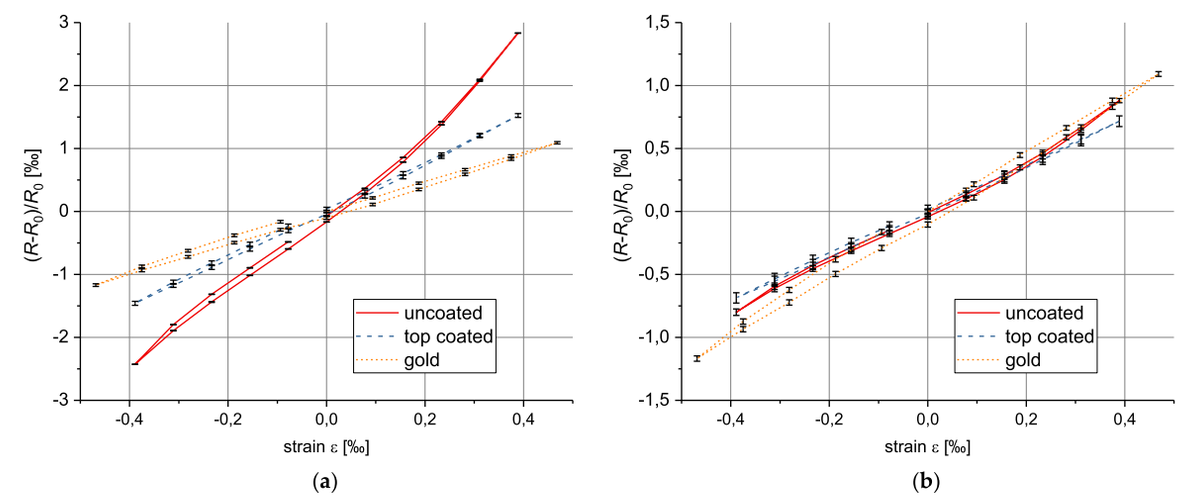

Fig. 9. (a) Comparison of carbon black based strain gauges, with (blue) and without (red) top coat and gold. (b) Comparison of silver based strain gauges with (blue) and without (red) top coat and gold. Both carbon black as well as silver show a non-vanishing hysteresis before and after top coating, which is bigger than the standard deviation of 100 measurement cycles each

the hysteresis is due to a mechanical behavior originating in the substrate, while the nonlinear effect has its origin in the polymer matrix of the strain gauge material itself. To confirm this, further mechanical investigations of the substrate are required.

6. Embedded piezo- and pyroelectric transducers

The polymer poly[(vinylidenefluoride-cotrifluoroethylene (P(VDF-TrFE)) enables the realization of flexible piezo- and pyroelectric transducers. Diluted in an appropriate solvent, it can be applied in many additive manufacturing processes, including, e.g., spray coating [25], inkjet printing [26], screen printing [5] and spin coating [27]. Recent applications include the fabrication of ultrasonic transducers [28], loudspeakers [14] and piezo- and pyroelectric sensor-matrix on plastic foil [5]. We have previously demonstrated the realization of the embedded piezo- and pyroelectric sensors in the organic coating of sheet steel [12]. In contrast to the sensors discussed above, the original primer-topcoat buildup has to be extended by three layers:

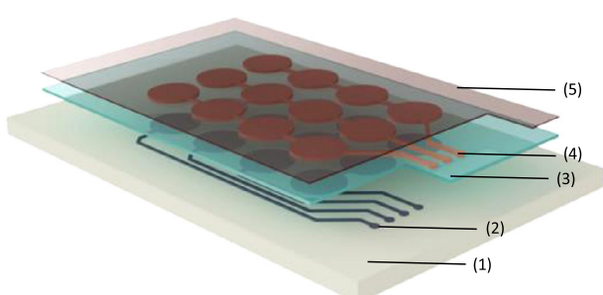

Fig. 10. Multilayer ferroelectric sensor stack design. (1) Substrate with organic coating. (2) Bottom electrode. (3) P(VDF-TrFE) ferroelectric intermediate coating. (4) Top electrode. (5) Organic top coating

a patterned bottom electrode, a P(VDF-TrFE) layer and a patterned top electrode (see Fig. 10). To generate the pyro- and piezoelectric

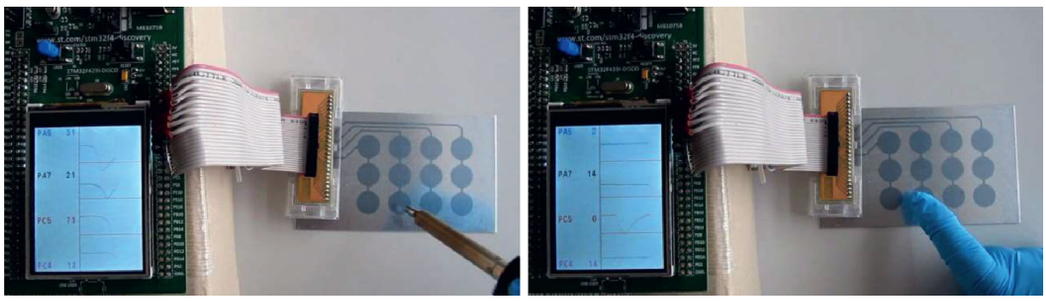

Fig. 11. Demonstration of the pyro- (left) and piezoelectric (right) properties of an early P(VDFTrFE) based prototype. The voltage response of the sensor is recorded with the ADC input of a STM32F4 microcontroller. The sensor consists of steel substrate, P(VDF-TrFE) layer and PEDOT:PSS top electrodes

properties of the P(VDF-TrFE) layer, high voltage poling, e.g., with a Sawyer-Tower circuit [29], is required. At peaks of the primer surface, very high electric field strengths may occur during the poling. To avoid electric breakdowns, the thickness of the P(VDF-TrFE) layer should be one order of magnitude higher than the root mean square surface roughness of the bottom electrode. The obtained piezoelectric coefficient after poling depends strongly on the applied electric field strength. To ensure a uniform piezoelectric coefficient in the layer, a uniform film thickness is important. A proof-of-principle realization of an early version of the concept is shown in Fig. 11. In this prototype, the P(VDF-TrFE) layer was spin coated on top of a steel substrate. The top electrodes were screen printed with PEDOT:PSS ink. The electric response was measured with the ADC input of a STM32F4 microcontroller. By moving a hot air gun over the sample the pyroelectric effect was demonstrated. As can be seen on the display in Fig. 11 (left), voltage pulses are generated in all four sensor elements. The piezoelectric effect is demonstrated by pressing an electrode with a glove-protected finger. The corresponding voltage peak can, again, be seen in the display (right).

7. Conclusion

Selected successful implementations of embedded transducers in the organic coating of sheet metal were reviewed. The devised concept has the potential to introduce additional functionality (e.g., touch, heat or strain sensing) to a variety of products without the need of significant changes to their existing implementation. In future work, efforts will particularly concentrate on the thorough characterization of material parameters as well as material behavior. Within this work thus far, it was demonstrated that printed transducers are a viable form of integration of monitoring and sensor structures into organic coatings on arbitrary surfaces with a non-negligible surface roughness.

Acknowledgements

Open access funding provided by Johannes Kepler University Linz. This work has been supported by the Linz Center of Mechatronics (LCM) in the framework of the Austrian COMET-K2 programme and the Austrian Research Promotion Agency FFG (project FFGP13310007).

References

1. Krebs, F. C., et al. (2009): A complete process for production of flexible large area polymer solar cells entirely using screen printing—first public demonstration. Sol. Energy Mater. Sol. Cells, 93(4), 422–441.
2. Ando, M., et al. (2015): Evidence for charge-trapping inducing polymorphic structural-phase transition in pentacene. Adv. Mater., 27(1), 122–129.
3. Allen, M., Lee, C., Ahn, B., Kololuoma, T., Shin, K., Ko, S. (2011): R2R gravure and inkjet printed RF resonant tag. Microelectron. Eng., 88(11), 3293–3299.
4. Jung, M., et al. (2010): All-printed and roll-to-roll-printable 13.56-MHz-operated 1-bit RF tag on plastic foils. IEEE Trans. Electron Devices, 57(3), 571–580.
5. Zirkl, M., et al. (2011): An all-printed ferroelectric active matrix sensor network based on only five functional materials forming a touchless control interface. Adv. Mater., 23(18), 2069–2074.
6. Altenberend, U., et al. (2013): Towards fully printed capacitive gas sensors on flexible PET substrates based on Ag interdigitated transducers with increased stability. Sens. Actuators B, Chem., 187, 280–287.
7. Maiwald, M., Werner, C., Zoellmer, V., Busse, M. (2010): INKtelligent printed strain gauges. Sens. Actuators A, Phys., 162(2), 198–201.
8. Sell, J. K., Enser, H., Jakoby, B., Hilber, W., Schatzl-Linder, M., Straus, B. (2015): Printed capacitive touch sensors embedded in organic coatings on sheet steel. In Proceedings of 2015 IEEE SENSORS (pp. 4–7).
9. Sell, J. K., Enser, H., Jakoby, B., Schatzl-Linder, M., Strauss, B., Hilber, W. (2016): Printed embedded transducers: capacitive touch sensors integrated into the organic coating of metalic substrates. IEEE Sens. J., 16(19), 7101–7108.
10. Enser, H., Sell, J. K., Schatzl-linder, M., Strauß, B., Hilber, W., Jakoby, B. (2017): Hysteresis and material effects of printed strain gauges embedded in organic coatings. In Eurosensors proc. 2017 (Vol. 1, pp. 624–627).
11. Enser, H., et al. (2018): Printed strain gauges embedded in organic coatings—analysis of gauge factor and temperature dependence. Sens. Actuators A, Phys., 276, 137–143.
12. Enser, H., et al. (2017): Concept for printed ferroelectric sensors on coated metallic substrates. In Proceedings of IEEE SENSORS.
13. Sandström, A., Asadpoordarvish, A., Enevold, J., Edman, L. (2014): Spraying light: ambient-air fabrication of large-area emissive devices on complex-shaped surfaces. Adv. Mater., 26(29), 4975–4980.
14. Hübler, A. C., Bellmann, M., Schmidt, G. C., Zimmermann, S., Gerlach, A., Haentjes, C. (2012): Fully mass printed loudspeakers on paper. Org. Electron., Phys. Mater. Appl., 13(11), 2290–2295.
15. Tobjörk, D., Österbacka, R. (2011): Paper electronics. Adv. Mater., 23(17), 1935–1961.
16. Van Osch, T. H. J., Perelaer, J., De Laat, A. W. M., Schubert, U. S. (2008): Inkjet printing of narrow conductive tracks on untreated polymeric substrates. Adv. Mater., 20(2), 343–345.
17. Khan, S., Dang, W., Lorenzelli, L., Dahiya, R. (2015): Flexible pressure sensors based on screen-printed p(VDF-TrFE) and p(VDF-TrFE)/MWCNTs. IEEE Trans. Semicond. Manuf., 28(4), 486–493.
18. Zymelka, D., Yamashita, T., Takamatsu, S., Itoh, T., Kobayashi, T. (2017): Printed strain sensor with temperature compensation and its evaluation with an example of applications in structural health monitoring. Jpn. J. Appl. Phys., 56(E5EC02), 1–5.
19. Hay, G. I., Evans, P. S. A., Harrison, D. J., Southee, D., Simpson, G., Harrey, P. M. (2005): Characterization of lithographically printed resistive strain gauges. IEEE Sens. J., 5(5), 864–870.
20. Latessa, G., Brunetti, F., Reale, A., Saggio, G., Di Carlo, A. (2009): Piezoresistive behaviour of flexible PEDOT:PSS based sensors. Sens. Actuators B, Chem., 139(2), 304–309.

21. Kang, I., Schulz, M. J., Kim, J. H., Shanov, V., Shi, D. (2006): A carbon nanotube strain sensor for structural health monitoring. Smart Mater. Struct., 15(3), 737–748.
22. Lang, U., Rust, P., Dual, J. (2008): Towards fully polymeric MEMS: fabrication and testing of PEDOT/PSS strain gauges. Microelectron. Eng., 85(5–6), 1050–1053.
23. Rausch, J., Salun, L., Griesheimer, S., Ibis, M. (2011): Printed piezoresistive strain sensors for monitoring of light-weight structures. In TEST conf. 2011.
24. Enser, H., et al. (2016): Printed strain gauges embedded in organic coatings. Proc. Eng., 168, 822–825.
25. Danz, R., Elling, B., Büchtemann, A., Mirow, P. (2002): Preparation, characterization and sensor properties of ferroelectric and porous fluoropolymers, In Proceedings of the 11th int. symp. electrets, (pp. 199–202).
26. Haque, R. I., Vié, R., Germainy, M., Valbin, L., Benaben, P., Boddaert, X. (2016): Inkjet printing of high molecular weight PVDF-TrFE for flexible electronics. Flex. Print. Electron., 1(1), 015001.
27. Tseng, H. J., Tian, W. C., Wu, W. J. (2013): P(VDF-TrFE) polymer-based thin films deposited on stainless steel substrates treated using water dissociation for flexible tactile sensor development. Sensors (Basel), 13(11), 14777–14796.
28. Ohigashi, H., Koga, K., Suzuki, M., Nakanishi, T., Kimura, K., Hashimoto, N. (1984): Piezoelectric and ferroelectric properties of P(VDF-TrFE) copolymers and their application to ultrasonic transducers. Ferroelectrics, 60(1), 263–276.
29. Sawyer, C. B., Tower, C. H. (1930): Rochelle salt as a dielectric. Phys. Rev., 35(3), 269–273.

Authors

Herbert Enser
received the B.Sc. degree in Technical Physics and the Dipl.-Ing. (M.Sc.) degree in Nanoscience and Technology from Johannes Kepler University (JKU) Linz, Austria, in 2014 and 2015, respectively. Since 2015, he has been a University Assistant with the Institute for Microelectronics and Microsensors, JKU, to attain his Ph.D. His research focus is on printed thin-film transducers and functional sensor materials.

Johannes K. Sell
studied Physics at the University of Wuerzburg, Germany, where he received his diploma in 2008. Since October 2008 he has been working at the Institute for Microelectronics and Microsensors of the Johannes Kepler University, Linz, Austria. There, he is currently focused on research in the field of printed embedded transducers.

Pavel Kulha
received a M.Sc. degree in electronic engineering in 2002 and a Ph.D. degree in microelectronics in 2009, both from the Czech Technical University in Prague, Czech Republic. Since 2003 he has been assistant professor at the Department of Microelectronics, FEE CTU in Prague. Since 2016, he has been with the Institute for Microelectronics and Microsensors, Johannes Kepler University, Linz, Austria, as postdoc researcher. His research interests include the design, modeling, development and applications of microsystems and microsensors.

Wolfgang Hilber
received the Dipl.-Ing. (M.Sc.) degree in physics and the Doctoral (Ph.D.) degree in technical sciences from the Johannes Kepler University (JKU), Linz, Austria, in 1993 and 1997, respectively. From 1994 to 1998, he was a research assistant with the Institute of Semiconductor and Solid State Physics, JKU. From 1998 to 2000, he collaborated in several research projects dealing with in-line process control for semiconductor manufacturing processes. In 2000, he joined the R&D division of E+E Electronics GmbH, Engerwitzdorf, Austria. There he conducted development projects in thin-film sensor technology, mainly for automotive applications, until he finally joined the Institute for Microelectronics and Microsensors, Johannes Kepler University Linz.

Bernhard Jakoby
obtained his Dipl.-Ing. (M.Sc.) in communication engineering and his doctoral (Ph.D.) degree in electrical engineering from the Vienna University of Technology (VUT), Austria, in 1991 and 1994, respectively. In 2001 he obtained a venia legendi for Theoretical Electrical Engineering from the VUT. From 1991 to 1994 he worked as a Research Assistant at the Institute of General Electrical Engineering and Electronics of the VUT. Subsequently, he stayed as an Erwin Schrödinger Fellow at the University of Ghent, Belgium, performing research on the electrodynamics of complex media. From 1996 to 1999 he held the position of a Research Associate and later Assistant Professor at the Delft University of Technology, The Netherlands, working in the field of microacoustic sensors. From 1999 to 2001 he was with the Automotive Electronics Division of the Robert Bosch GmbH, Germany, where he conducted development projects in the field of automotive liquid sensors. In 2001 he joined the newly formed Industrial Sensor Systems group of the VUT as an Associate Professor. In 2005 he was appointed Full Professor of Microelectronics at the Johannes Kepler University Linz, Austria. He is currently working in the field of liquid sensors and monitoring systems.